



GIS-based revised universal soil loss equation for estimating annual soil erosion: a case of lower Kulsī basin, India



G. Thakuria¹ 

Received: 26 November 2022 / Accepted: 8 February 2023

Published online: 15 February 2023

© The Author(s) 2023, corrected publication 2023 [OPEN](#)

Abstract

Assessment and estimation of soil loss is a fundamental aspect of land and water resource conservation and management practices as it provides necessary information in the course of watershed-level development of a region. The soil loss model of Wischmeier and Smith, popularly known as the Revised Universal Soil Loss Equation, was selected to estimate soil loss in the lower Kulsī river basin due to its simplicity, versatility, and flexibility nature method in the Geographic information system platform. Most original governmental datasets, mainly daily gauge rainfall from 2009 to 2018, satellite images for land use land cover, digital elevation model of Shuttle Radar Topographic Mission for topographic factor, and National Bureau of Soil Survey and Land-use Planning, India soil map were utilized to estimate the average annual soil erosion. The estimated average annual soil erosion ranges from 0.0 to 6.45 thousand $t\ ha^{-1}y^{-1}$, grouped into low, moderate, high, and very high risk of soil erosion. A basin area of 36.235 km^2 (1.85%) basin area was identified as high to very high zones of soil erosion risk and needed immediate conservation measures to reduce the erosion risk.

Article highlights

- (1) The soil loss estimate is vital for taking appropriate anti-erosion measures and enhancing surface runoff in identifying priority areas.
- (2) The GIS-based RUSLE model is a simple and widely acceptable soil loss estimating model for the watershed in a tropical monsoon climate.
- (3) Rainfall erosivity, conservation practice, and topographic factors of the basin contribute more to soil erosion.

Keywords Soil erosion · Geographical information system (GIS) · Land use land cover (LULC) · Revised Universal Soil loss equation (RUSLE)

1 Introduction

Soil erosion is a process of land degradation caused by a mixture of natural determinants such as topography, soil, climatic, and vegetation cover, and human interference

like agricultural practices, deforestation, land modification, and construction activities [1]. Soil erosion is a severe problem with inestimable economic and environmental impacts worldwide because of its extent, magnitude, rate, and complex processes [2]. Accurate

✉ G. Thakuria, gitika.thakuria@cottonuniversity.ac.in | ¹Geography, Cotton University, Guwahati 781001, India.



assessment and soil loss estimation are crucial in sustainable land and water resources management. Various soil erosion model has been developed to estimate soil erosion. The Universal Soil Loss Equation (USLE), the Modified Universal Soil Loss Equation (MUSLE), and the Revised Universal Soil Loss Equation (RUSLE), the Revised Universal Soil Loss Equation version 2 (RUSLE 2) are the most famous empirical models of soil loss applied worldwide [3, 4]. The soil loss model, namely the Universal Soil Loss Equation (USLE), was developed by W. H. Wischmeier and D.D. Smith in 1978. It is a widely used standard mathematical model to predict long-term average annual soil loss on arable land [5]. With its revised (RUSLE) and modified (MUSLE) [5, 6], the USLE is still being used in many studies [7].

The RUSLE model is relevant for ecosystem services related to soil erosion and protection as the model can predict erosion potential on a cell-by-cell basis [8]. It is effective to identify the spatial pattern of the annual soil loss within a catchment scale. The method has been applied in many worlds regime and has proven effective in estimating soil loss [9]. The algorithms can be implemented using standard GIS software based on literature values or adapted to empirical data. GIS can be used to isolate and query location to identify the role of individual variables contributing to the observed erosion potential value [7]. A bundle of research work has been done on the estimation of long-term soil loss using geospatial techniques in the world, such as the Fincha Catchment of Ethiopia [12], the Dolapha district of Nepal [13], the Kalu Ganga River Basin [14], and Pabaragamuwa Province [15] of Sri Lanka, the Kelantan state, north-eastern Peninsular Malaysia [16], Wadi El Hayat watershed of Saudi Arabia [17], the Northwestern Crete in the semi-arid region of Greece [18], tropical mountain river basin of the southern Western Ghats [19], Padma River Basin, Siruvani River watershed in Attapady valley, Kerala [20], the Barakar River Basin of Jharkhand [21], the Kangsabati River Basin of eastern Chotanagpur Plateau [22], the Panchnoi River Basin [23], and the Dikrong River Basin in a hilly catchment of Northeast India [24] in India.

The Kulsi River basin of North-east India is exceptionally vulnerable to landslide and soil loss due to high seasonal rainfall increasing surface runoff in severe hill slopes, and terrain modification for human economic needs. Assessing soil loss in the basin is needed for land and water resources management and conservation programs. Therefore, the present study attempts to estimate the average annual soil loss in the lower Kulsi basin using RUSLE with the ArcGIS interface. The results of this research paper can help the decision-makers, and local government, with land and water resources planning to reduce erosion and environmental protection.

2 Methodology

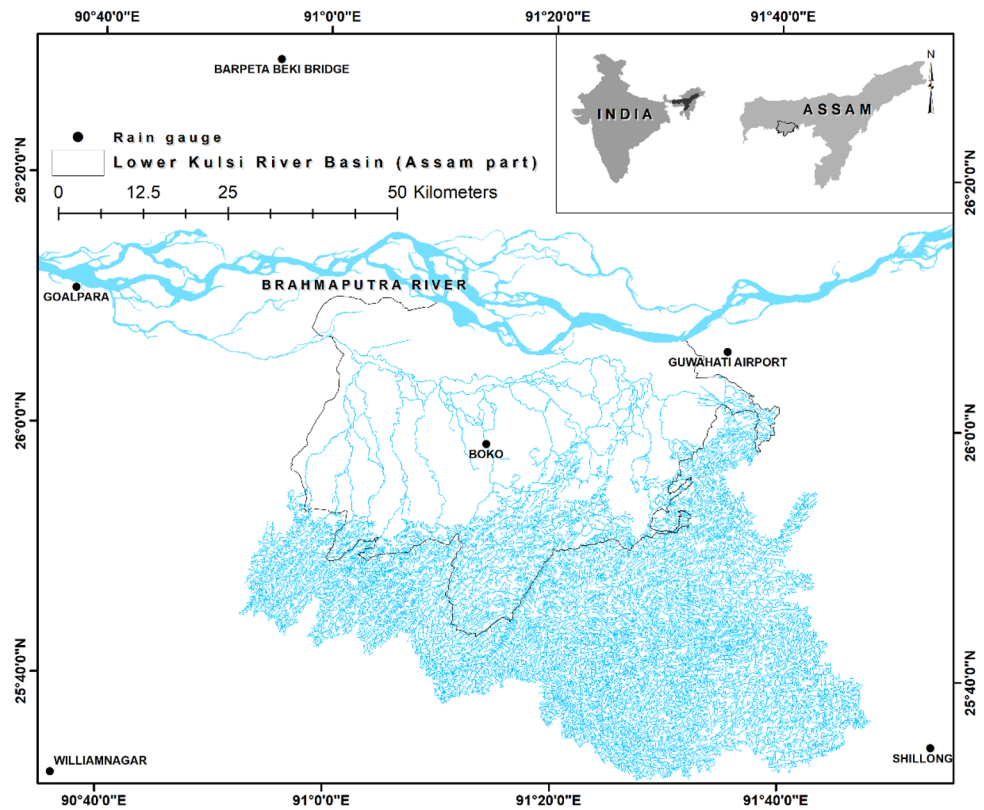
2.1 Study area

The Kulsi River is a left-bank tributary of the Brahmaputra River. It is on the northern front of the Shillong Plateau, a northward-flowing river system that drains Assam's plain region and joins into the Brahmaputra River. The river is known as Khri in Meghalaya, where the tributaries like Um Krisinya River, Um Siri, and Um Ngi confluence at Ukiam, after reaching the alluvial plain of Assam, the river is known as Kulsi River. The Kusli River basin has a total area of around 1953 km². Geographically, its latitude and longitudinal extension are 25°31'58.8" N to 26°75'3.33"N and 91°E to 91°48'30"E, showed in Fig. 1. The upper catchment of the study area is composed of moderate to highly dissected structural hills and valleys, which depict the surface runoff of the rugged hilltop and are affected by soil erosion. The debris slopes are moderate to steep and severely eroded with the high acceleration of finer alluvial soil. The catchment has elevations ranging from 80 to 1220 m. The topographic subunits of the low-lying plains are the young alluvial plain, the old alluvial plain, the active flood plain, and the older flood plain. The pediment complex is another crucial landform unit with a moderate slope sustaining natural vegetation and grassland. The upper catchment is mainly composed of fine soil texture soil, the parent material is Gneiss, and the downstream section of the river is covered mainly by alluvium. The upper catchment area belongs to the age of the Proterozoic structure, and the downstream belongs to the age of Meghalaya, formed during the Barpeta-I, Sorbhog, and Hauli formations.

The Kulsi is an 8th-order drainage basin located in the sub-tropical monsoon type of climatic zone with highly seasonal rainfall in summer. Average annual rainfall was recorded at 1956.67 mm at the Boko rain gauge station located in the central part of the basin. It received higher rainfall in the catchment area and decreased at the Guwahati airport station northeast. More than 74% of the rain occurs only in summer (May to September), causing surface runoff and vulnerability for soil erosion and landslide on the rugged topography in the catchment and flood inundation in the lowland. In addition, 38% of the study area was covered by agricultural land, and most of the natural vegetation was converted to arable land with traditional crop practices on hill slopes leading to soil erosion.

2.2 Database

The watershed of the Kulsi has been prepared from the survey of India's topographical sheets at a 1:50,000 scale. The watershed boundary is delineated after carefully digitizing

Fig. 1 Location map of the lower Kulsli River basin

the stream network in Arc GIS 10.6 software from topographic sheet no. 78 N/4, 78 N/8, 78 O/1, 78 O/2, 78 O/5, 78 O/6, 78 O/9, 78 O/10, and 78 O/14 covings 4135 km² area. Topographical sheets are registered in the WGS_1984_UTM_Zone_46N projection system before digitizing linear features like streams network and contour lines. The downstream of the watershed in the Assam part is extracted as a study area, namely the lower Kulsli River basin covering a 1956 km² area. The rainfall data were collected from RMC, Guwahati, and RSRS, Boko, for 2009–2018. The study area has only two rain gauge stations, Boko and Guwahati Airport. However, seven stations were used to estimate the rainfall distribution map more accurately. Tikirikila, Williamnagar, and Shillong rain gauge stations are located in Meghalaya Plateau towards the southern boundary of the basin. Goalpara and Beki River Barpeta rain gauge stations are located West and North West boundary of the study area. The soil map and its attribute information are extracted from the soil map prepared by NBSS & LUP, 1999. The LULC types of the study area are delineated from the satellite data (IRS LISS IV, DOP 26/01/2018) based on visual interpretation (digitized) techniques in the GIS environment. The satellite image is projected at the same coordinate system units, WGS_1984_UTM_Zone_46N. The current LULC patterns are digitized after carefully observing the features up to the 1:1000 scale using Arc GIS 10.6 software. The whole approach for preparing the LULC map

of the study area involved visual observation, preliminary interpretation using SOI topographical map and Google Earth satellite map provided by Landsat/Copernicus 2021, and final interpretation after a rigorous field check. The correctness of the LULC information derived from satellite images was assessed using the Kappa coefficient. There are 500 ground control points taken for the assessment. The Kappa coefficient was 0.828, indicating almost perfect strength of agreement between classified and ground truth data (see Table 1).

2.3 Method

The RUSLE model was used to estimate average annual soil loss to delineate the erosion-prone area in the lower Kulsli Basin. It is a straightforward, flexible, and widely acceptable model to estimate average annual soil erosion in a diverse land cover watershed. The estimated average annual soil erosion was quantified using Eq. 1 [5, 25].

$$A = R \times K \times L \times S \times C \times P, \quad (1)$$

where A means average annual soil loss per unit area (t ha⁻¹ y⁻¹), R is the rainfall erosivity (MJ mm ha⁻¹ y⁻¹), K is the soil erodibility factor (ha h MJ⁻¹ mm), L is the slope length factor, S is the slope steepness factor (dimensionless), C is

Table 1 Detailed of the database used in the study

Data	Description	Source
Toposheet	No 78 N/4, 78 N/8, 78 O/1, 78 O/2, 78 O/5, 78 O/6, 78 O/9, 78 O/10, and 78 O/14; Scale 1:50000 For Watershed, Streams network	Survey of India
Rainfall data	For 2009–2018 Seven rain gauges—Boko, Guwahati airport, Tikirikila, Goalpara, Beki, Williamnagar, and Shillong.	Regional Meteorological Centre (RMC), Guwahati, India. Regional Sericulture Research Stations (RSRS), Boko.
Soil map	Soil texture, 1999 Scale 1:50000	National Bureau of Soil Survey and Land-use Planning www.nbsslup.in
Satellite image	Resourcesat 2, LISS III 19/02/2018 24 m IRS LISS IV, 26/01/2018 5 m SRTM DEM 30 m	National Remote Sensing Center, Hyderabad www.bhuvan.nrsc.gov.in Earth explorer www.earthexplorer.co.in

the cover management factor (dimensionless), and P is the support and conservation practice factor (dimensionless).

Rainfall erosivity (R) power is the most dominating soil erosion factor in a watershed. This paper determined the watershed's rainfall erosivity from the ten years of recorded average annual rainfall (2009–2018) of seven rain gauge stations. The spatial distribution of rainfall was prepared using interpolate distance weighted (IDW) interpolation tools in the Arc GIS 10.5. IDW is the preferable method for measuring a river basin's smooth rainfall distribution in terms of mean error [26]. The resultant grid map was integrated into the empirical Eq. 2 developed by Ram et al. using a raster calculator to generate the rainfall erosivity factor for the Indian framework [27].

Rainfall erosivity,

$$R = 81.5 + 0.38P, \quad (2)$$

Where R is the rainfall erosivity factor ($\text{MJ mm ha}^{-1} \text{h}^{-1} \text{year}^{-1}$), and P is annual precipitation for areas where annual precipitation ranges between 340 and 3500 mm.

Soil erodibility factor (K) denotes the susceptibility of soil to erosion determined by the texture of the soil, grain size, structural integrity, organic content, drainage potential, and cohesiveness [20]. The soil texture map and the attribute information of the study area are collected from the soil map prepared by the National Bureau of Soil Survey and Land Use Planning (NBSS, 1999). K factors for each soil texture of the study were identified from the soil erodibility table after Stone and Hilborn by considering less than 2% organic matter content [28]. The K value of each soil texture was added to the attribute table and converted into a raster layer in the ArcGIS platform.

The topography of landform plays a significant role in soil loss as it changes more rapidly with the slope steepness and length. The topographic factor is the product of slope length (L) and steepness (S). It affects soil erosion and is accounted for by the RUSLE model to estimate average annual soil loss. This paper quantified the combined LS factor using Eq. 3, proposed by Moore and Burche [29].

$$LS = \left(\text{flow accumulation} \times \frac{\text{Cell size}}{22.13} \right)^{0.4} \times \left(\frac{\text{Sin slope}}{0.0896} \right)^{1.3}, \quad (3)$$

Where flow accumulation is the accumulated upslope contributing area for a given cell, cell size means the area covered by each grid; Sin slope is the Sin value of slope degree. The flow accumulation and the slope map of the study area were generated from SRTM DEM of 30 m using hydrological and surface extension in the ArcGIS platform. The combined LS factor was computed by Eq. 3 using the raster calculator of ArcGIS spatial analysis extension.

Cover management factor (C) is another crucial factor for soil erosion: vegetation cover, cropping pattern, soil productivity, and subsurface biomass can resist soil erosion after the rainfall event. Wischmeier and Smith defined the C factor as the ratio of soil loss from land cropped under specified conditions to the corresponding loss from clean-tilled, continuous fallow land [5]. Remote sensing data can quickly assess the generation of the C factor by using the normalized difference vegetation index (NDVI). It is a dimensionless index that can estimate vegetation strength and describes the difference between visible and near-infrared reflectance of vegetation cover [30]. In this paper, the NDVI indicator

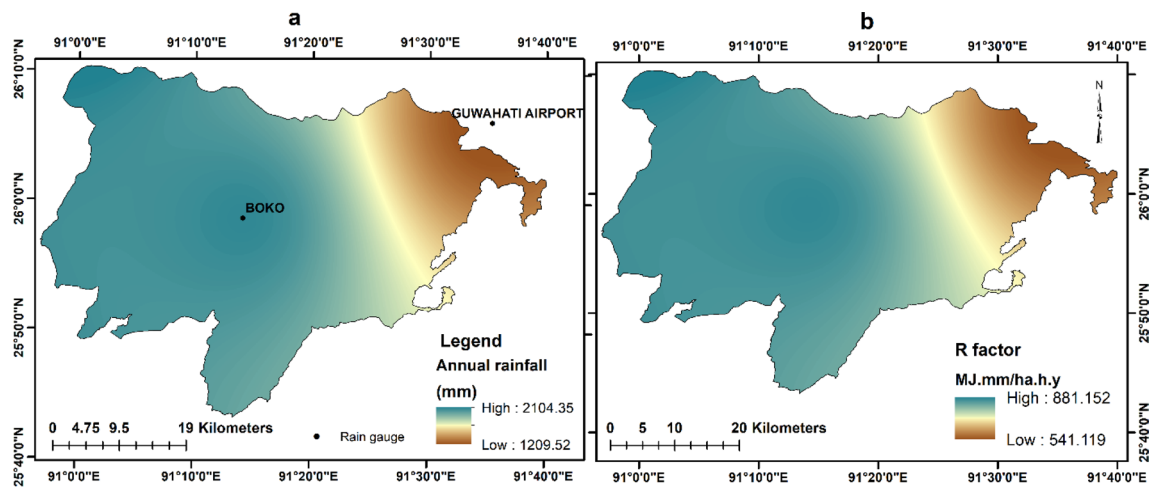


Fig. 2 **a** Spatial distribution of total annual rainfall in mm (2018), **b** R factor map of the lower Kulsli River basin

is integrated into the following Eq. 4 to generate the C factor value [18, 31, 32].

$$C = \exp\left(-\alpha \times \frac{NDVI}{\beta - NDVI}\right), \quad (4)$$

where α and β are the parameters that determine the shape of the curve relating to NDVI and C factors, Van der Knijff et al. supposed the value of 2 and 1 for α and β , respectively, for good results and successfully applied to obtain C factor [31].

A support practice factor (P) map was generated based on the LULC map of the study area. Current LULC categories were delineated through a systematic visual interpretation of high-resolution satellite images. The study area is classified into ten main types of LULC, namely barren land, cropland tea plantation, forest, grassland, shrubland, marshy land, exposed rocky surface, water bodies, and built-up land (Fig. 6). P values of each LULC category were added to the attribute table and converted to the raster layer in the ArcGIS platform. P-value is a dimensionless parameter. It ranges from 0 to 1. The highest value denotes no conservation practices (barren land), and the minimum values are assigned for built-up and other conservation practices with contour cropping [20].

3 Results and discussions

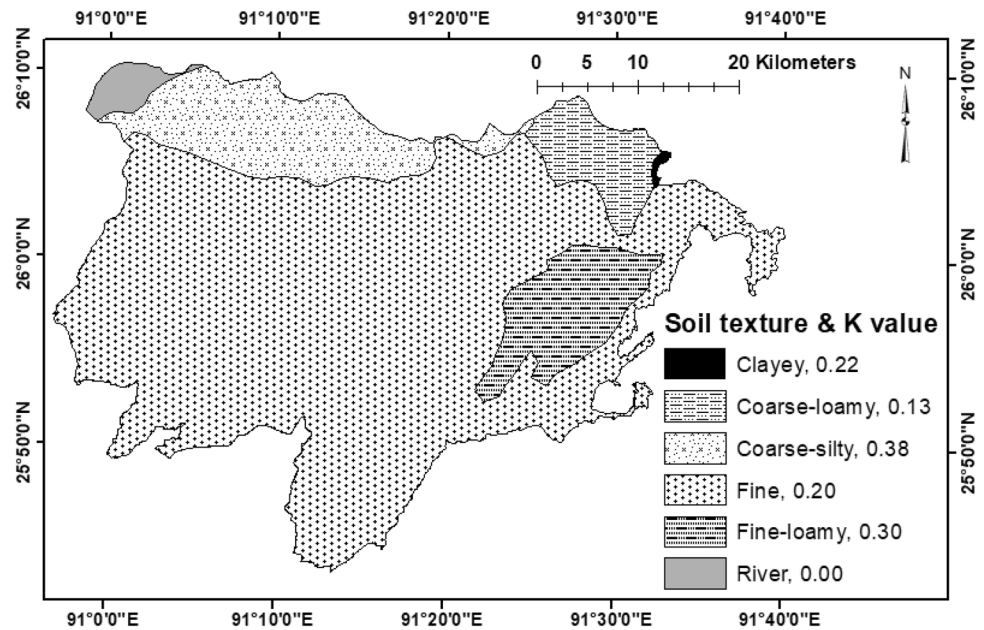
The average annual soil loss of the lower Kulsli basin was estimated based on the product of five erosion factors of the RUSLE model, rainfall erosivity factor (R), soil erodibility factor (K), topographic factor (LS), cover management (C), and conservation practice (P). Many factors affect soil erosion in tropical and sub-tropical areas. One

of the contributing factors is heavy rainfall which leads to rain splash, surface runoff, and soil erosion [33]. Rainfall and runoff in the hilly area trigger mass movement and landslides [2, 34]. The 10 years (2009–2018) mean annual rainfall of seven rain gauge station data was used to compute the R factor. The average annual rainfall during the periods varies from 1209 to 2104 mm (Fig. 2a), and the corresponding rainfall erosivity factor of the study area ranges from 541 to 881 MJ mm ha⁻¹ h⁻¹ y⁻¹ (Fig. 2b). The higher R-value designates higher rainfall to contribute to soil erosion [35]. More than 74% of the total annual rainfall of the basin occurs only in the summer months from May to September. Such highly seasonal rainfall contributes surface runoff and is susceptible to soil erosion in hills and floods in the lowland.

The soil texture of the study area is grouped into five categories—clay, coarse silt, coarse loam, fine loam, and fine. Figure 3 illustrates the soil texture and corresponding K factor values identified from the soil erodibility table after Stone and Hilborn (2000). K value of the basin varied from 0.13 t h MJ⁻¹ mm⁻¹ of coarse loam texture soil to 0.38 t h MJ⁻¹ mm⁻¹ of coarse grain silt texture soil. The soil erosion susceptibility increases with a higher K factor [36]. The high K factor of silt soil is more susceptible to erosion than the lower K factor of loam and clay soil in the lower Kulsli basin.

The slope length (L) and steepness (S) provide terrain analysis quantitatively of a basin. The study area's topographic factor map (Fig. 4c) is prepared based on two topographic parameters, flow accumulation and slope (%), using Eq. 3. The flow accumulation layer is generated by calculating the flow direction of DEM using hydrological extension tools in ArcGIS. Figure 4a shows greater flow accumulation values and specifies the area to form more accessible runoff. The basin slope ranges from 0° to

Fig. 3 Soil texture map and corresponding erodibility factor (K) value



64° or 207% (Fig. 4b). A higher value of flow accumulations and slopes in the basin creates a higher value of the topographic factor and makes it susceptible to soil erosion [37]. The basin area's topographic factor (LS) varies from 0 to 80. Figure 4c demonstrates the spatial variation of the LS factor in the study area.

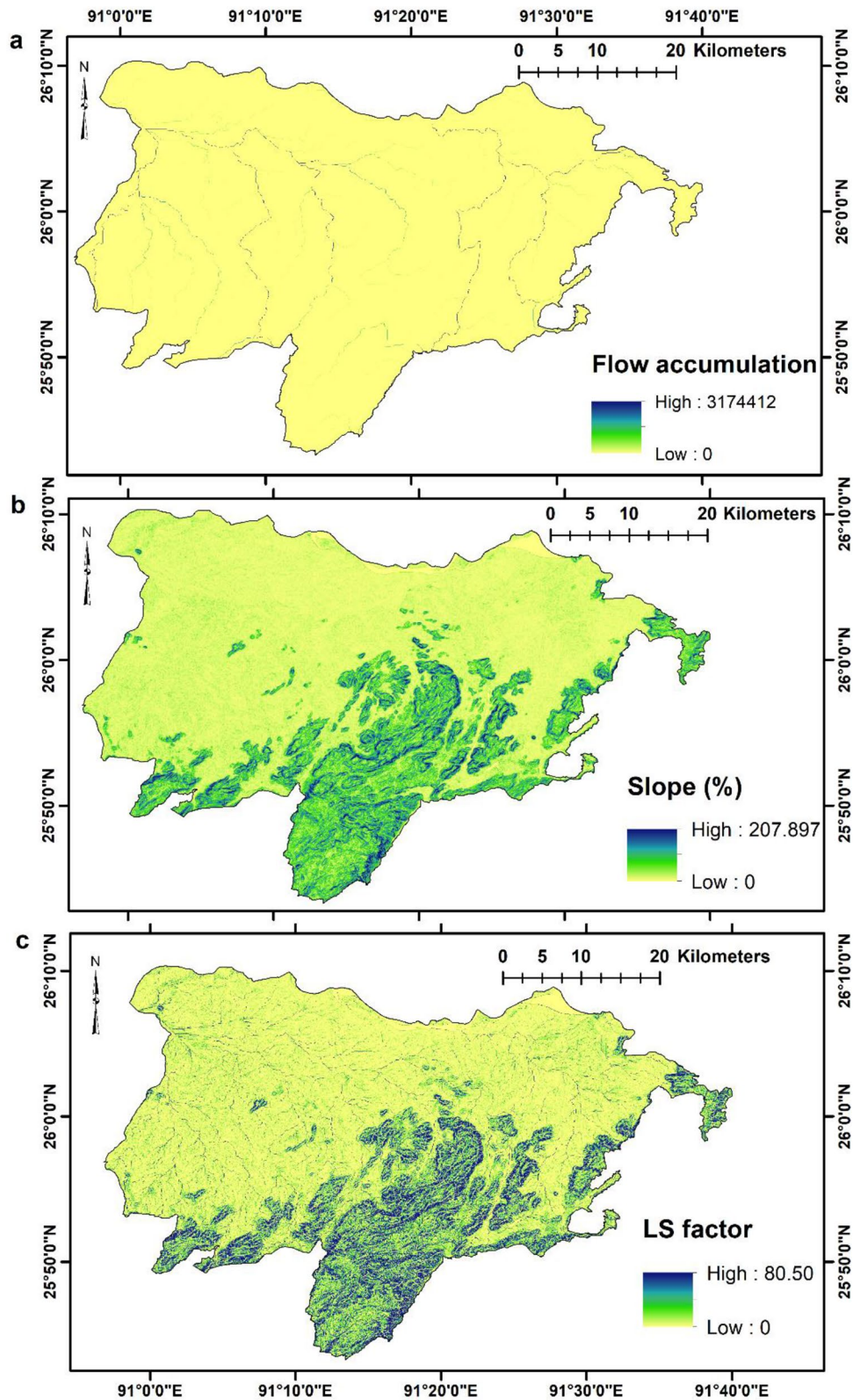
The cover management and support practice factors are the dimensionless parameters of the RUSLE model, derived from current land use and land cover of the lower Kulsu River Basin. The cover management factor is derived from the NDVI map using Eq. 4. NDVI is a dimensionless parameter used to estimate the density of vegetation. It ranges from 0.07 to 0.37 (Fig. 5a). A high value of NDVI indicates dense forest, and a low value below 0.1 signifies bare surface cover and susceptibility to soil erosion. The estimated C factor of the area varies from 0.29 to 0.85 (Fig. 5b). The C factor value nearer to zero means well protected, while the value approaches 1 for barren land [7].

The study area's land use and land cover map were prepared from satellite images based on visual interpretation techniques (Fig. 6) for identifying the support practice (P) factor. It is a dimensionless factor, and the value will be 0–1, 0 for good conservation practices and 1 for poor conservation practices. The study area is classified into ten land use/land cover categories: agricultural land, tea plantation, forest, shrub forest, trees mixed with grassland, marshy land, barren land, exposed rocky surface, water bodies, and built-up land. Agricultural land occupied 38.65% of the total study area, comprising single crops in the lowland (36.65), double crops in the highland (1.91%), and tea plantations (only 0.087%) in the foothills area of the basin. Lower P values were assigned for the cropland.

Cultivable fallow, built-up, and barren land was mainly responsible for excess soil erosion and higher P-value. About 566 km² of the watershed covered by natural vegetation like Sal and Teak in the low-lying area was identified as less susceptible to soil erosion and assigned a low P-value.

The estimated average soil loss of the lower Kulsu basin was quantified by integrating all factor layers of RUSLE using the raster calculator of ArcGIS. The resultant soil loss map is presented in Fig. 7. It is estimated that the average annual soil loss of the lower Kulsu River basin varied from 0 to 6.453 thousand t ha⁻¹y⁻¹, with the mean of the range being 0.25 t ha⁻¹y⁻¹. Table 2 illustrates the four categories of the annual average rate of soil erosion namely, low (0–1 t ha⁻¹y⁻¹), moderate (1–10 t ha⁻¹y⁻¹), high (10–100 t ha⁻¹y⁻¹), and very high (above 100 t ha⁻¹y⁻¹). A large portion of the basin was classified as erosion-free or with very low soil erosion. It occupied a 1343 km² area and was more than 68% area of the basin. About 29.36% of the total area was categorized into a moderate level of soil erosion (1–10 t ha⁻¹y⁻¹), 1.80% area had a high level of soil erosion (10–100 t ha⁻¹y⁻¹), and 1.005 km² area of the basin was susceptible to a very high level of soil erosion (above 100 t ha⁻¹y⁻¹). Table 3 illustrates the estimated mean of soil erosion and their supportive factor values on different land use/land cover classes. Due to the high P and LS factors, the high mean value of soil erosion in the basin was observed on the barren and forest on hills, including cultivable fallow land and marshy land in the catchment area. Most of the vegetation cover in the basin is grown on high-gradient topography. Built-up and exposed rocky surfaces on hills (Fig. 8) were also identified as high-risk areas of

Fig. 4 **a** Flow accumulation map, **b** the slope (%) map is prepared from SRTM DEM, **c** LS factor map of the study area is prepared based on flow accumulation and slope map using the Eq. 3 in raster calculator



soil erosion with an estimated mean value of soil erosion greater than $1.75 \text{ t ha}^{-1} \text{ y}^{-1}$ and $1.57 \text{ t ha}^{-1} \text{ y}^{-1}$, respectively. The high LS factor is mainly responsible for the increased risk of soil erosion in forest cover.

Literature shows that the average soil loss of less than $1 \text{ t ha}^{-1} \text{ y}^{-1}$ is considered the tolerable soil erosion rate [25]. However, the findings of the soil loss rate in different land use of the Kushi basin were considered above

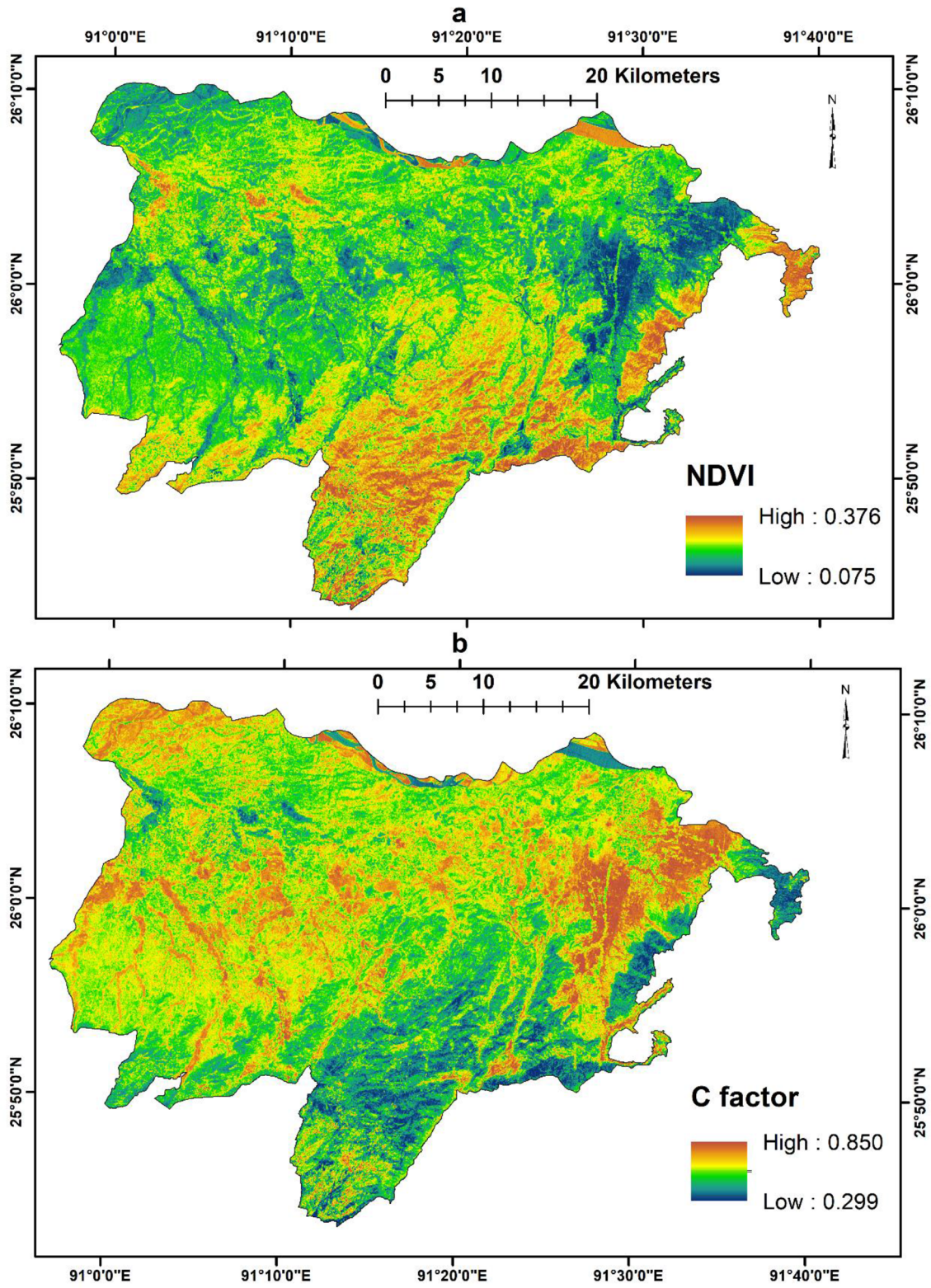


Fig. 5 a Normalized difference vegetation index map, b C factor map

Fig. 6 Land use and land cover map and corresponding support practice factor

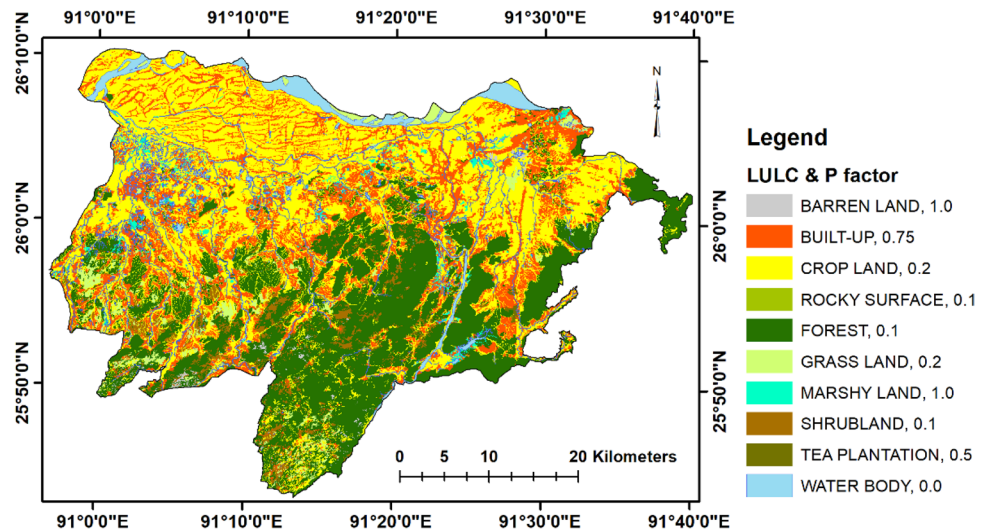


Table 2 Average annual soil loss of the lower Kulsu River basin

The severity of soil loss	Rate of soil loss (t ha ⁻¹ y ⁻¹)	Area (km ²)	Area (%)
Low	0–1	1343.93	68.78
Moderate	1–10	573.65	29.36
High	10–100	35.23	1.80
Very high	100 <	1.005	0.05

the tolerable rate except for shrub vegetation. Any soil loss above 1 t ha⁻¹y⁻¹ was considered irreversible soil erosion [38]. FAO 2015 shows average soil erosion rate for a tropical region is often less than 10 t ha⁻¹y⁻¹ [39]. However, the resultant spatial variation of soil loss from 0 to 6453 t ha⁻¹y⁻¹ in the lower Kulsu basin indicates a higher soil erosion rate than the average of the tropical region. Much catastrophic soil loss was estimated in the tropical climatic region of India by the findings ranges 0–10^{5.578} t ha⁻¹y⁻¹ in the tropical southern Western Ghats of Kerala [19], 473,339 t/y in the Nethravathi basin of Karnataka [7], 0–250 t ha⁻¹y⁻¹ in the Indian Himalaya region of Uttarakhand [39]. These estimated values of soil loss are quite higher than those in other countries of the world. The results of the average soil loss have been compared with the past literature of various catchments across the world, including the findings of estimated soil loss ranges 0.0–76.5 t ha⁻¹y⁻¹ in the Fincha catchment of Ethiopia [40], 7.6–90 t ha⁻¹y⁻¹ in the Wadi El Hayat watershed of Saudi Arabia [17], 0.0–4.66 t ha⁻¹y⁻¹ in the Kalu Ganga watershed [14] and 0.0–50 t ha⁻¹y⁻¹ in the Sabaragamuwa Province of Sri Lanka [15], 0–120 t ha⁻¹y⁻¹ in sub-Saharan Africa [41], 0–150 t ha⁻¹y⁻¹ in

Alaca catchment of Turkey [42], 4.3–1819.7 t ha⁻¹y⁻¹ in the Yangou watershed in Loess Plateau, China [43], 0–18473 t ha⁻¹y⁻¹ in the Pansoon sub-basin of Malaysia [44]. It has been proved that India’s soil erosion problem is much more catastrophic than other countries.

About 36.23 km² of the study area is sensitive to the soil erosion rate of more than 10 t ha⁻¹y⁻¹ because of the bare ground, cultivable fallow in the hilly topography. The field observation of highly erodible bare ground on the hills is exemplified in Fig. 9. Figure 10 shows the aerial view of the erodible barren land on Bandaraja Hill in the study area, where the soil loss rate was estimated at more than 100 t ha⁻¹y⁻¹. The soil particle on such surfaces will be detached by extreme seasonal rainfall with high rill erosion and landslide content. Support practice (P) and topographic factor (LS) with cover management are the leading factors that contribute to massive soil loss even in the same rainfall erosivity (R) and soil erodibility (K) factors for the study area. About 5.24 km² of bare ground and cultivable fallow land on the hill with a fine loam soil texture area is identified most severe soil loss and needs instantaneous action for conservation. In this research, the spatial soil erosion content was measured using high-resolution satellite data (5 m) for the first time with reasonable accuracy of the LULC map for measuring the P factor. Seven observed gauge rainfall was used for calculating rainfall erosivity and SRTM DEM with 30 m spatial resolution for calculating LS factor. The GIS-based RUSLE model has successfully estimated long-term average annual soil erosion in the lower Kulsu River Basin. The model offers us a valuable means for identifying the susceptible area of soil loss for planning and implementing soil and water conservation measure to reduce the soil loss. The results can be improved by

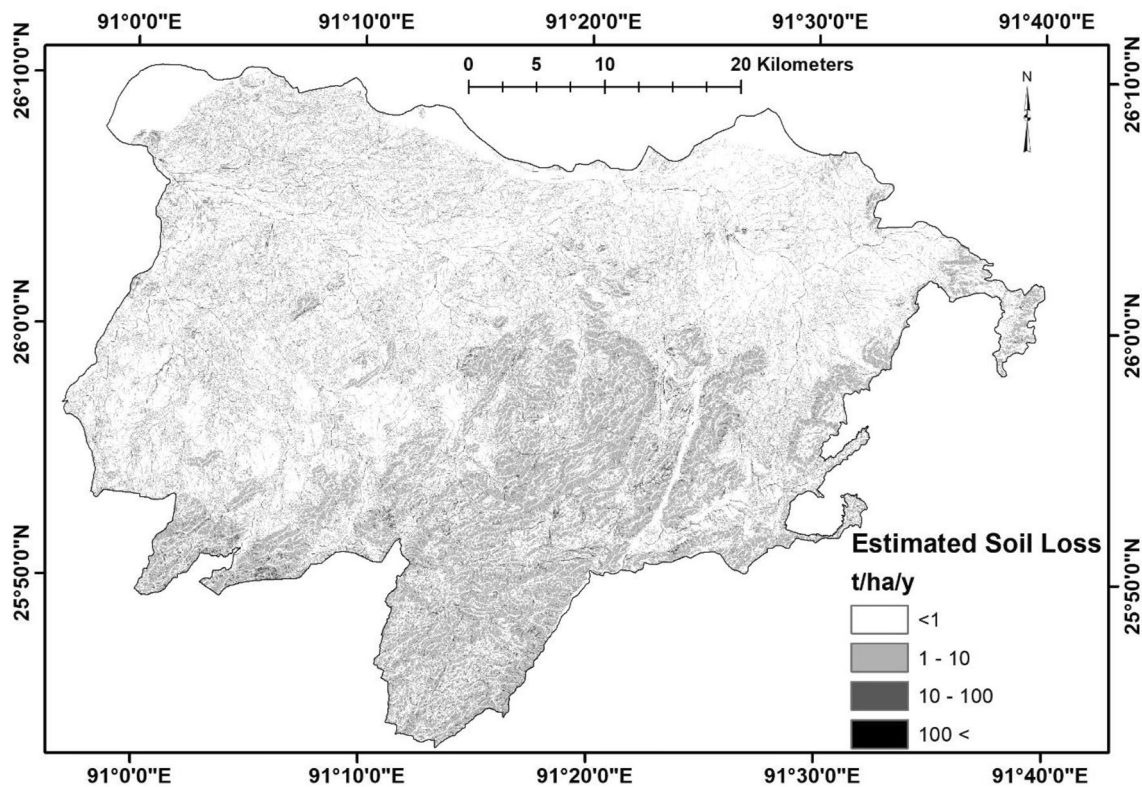


Fig. 7 Estimated soil loss map of the lower Kushi River Basin based on the RUSLE model

Table 3 Mean the value of soil erosion supporting factors on different land use/land cover classes of the study area

Land use/land cover	Area (km ²)	Rainfall erosivity, R (MJ mm ha ⁻¹ h ⁻¹ y ⁻¹)	Soil erodibility, K (t h MJ ⁻¹ mm ⁻¹)	Slope length and steepness, LS	Cover management, C	Support practice, P	Mean soil loss (t ha ⁻¹ y ⁻¹)
Barren land	7.24	801.12	0.195	0.154	0.527	1.0	11.72
Cropland	754.39	797.16	0.232	0.054	0.579	0.2	1.09
Forest	566.88	801.99	0.208	0.204	0.496	0.1	1.67
Grassland	51.60	806.31	0.228	0.064	0.558	0.2	1.23
Marshy land	27.66	803.39	0.201	0.058	0.536	1.0	4.71
Built-up	393.52	791.82	0.221	0.028	0.562	0.75	1.75
Waterbody	86.21	794.80	0.000	0.102	0.556	0.0	1.25
Shrubland	66.93	838.75	0.203	0.136	0.531	0.1	0.25
Rocky surface	0.52	594.34	0.198	0.222	0.587	0.1	1.57
Tea plantation	1.71	725.27	0.254	0.023	0.580	0.5	1.30

improving the input data, like a high-resolution DEM, to extract a more accurate LS factor. More rainfall stations within the study area can improve the accuracy of the R factor and a more accurate assessment of soil erosion of the basin.

4 Conclusion

Highly varied topographic with cover management factors (C) and support for the practice (P) of land use and land covers were the main factors for soil erosion in the basin. Barren land, exposed rocky surface land & stone



Fig. 8 Most sensitive soil erosion on the exposed surface near the Rani area of the lower Kulsī basin (image collected by the author from the field)



Fig. 9 Highly erodible bare ground on Bandaraja Hill of the lower Kulsī basin (image collected by the author from the field)



Fig. 10 Aerial view of the highly erodible barren land on the Bandaraja Hill in the Kulsī basin. Source: Esri, Maxer, Earthstar Geographics, and the GIS Community

mining, and cultivable fallow land on the hilltop area are mainly responsible for excess soil erosion during the rainy season. Besides high-intensity rainfall, soil characteristics and cover management are equally important contributing factors to soil erosion. About 1.85% area of the basin was identified as a highly susceptible zone of soil erosion. The zone's estimated rate of soil erosion was above $10 \text{ t ha}^{-1}\text{y}^{-1}$. The area primarily comprises cultivable fallow land, barren land, streams, and vegetation cover of hilly terrain. Therefore, the area needs immediate attention to soil conservation measures to reduce soil erosion. Indeed, the study demonstrated that the simple, flexible, and cost-effective GIS-based RUSLE model could facilitate long-term estimation in an upland-lowland watershed. Hence, the resultant research can be applied to watershed management, land and water resource action plans, and water harvesting site delineation to reduce soil erosion.

Acknowledgements The author would like to express her gratitude to the Science and Engineering Research Board (SERB) for its financial support for this project. Special thanks to the Scientists of the Regional Sericulture Research Station (RSRS), Boko, for providing rainfall and other meteorological data.

Data availability Data will be made available on reasonable request.

Declarations

Conflict of interest The author has no financial or non-financial interests to disclose.

Open Access This article is licensed under a Creative Commons Attribution 4.0 International License, which permits use, sharing, adaptation, distribution and reproduction in any medium or format, as long as you give appropriate credit to the original author(s) and the source, provide a link to the Creative Commons licence, and indicate if changes were made. The images or other third party material in this article are included in the article's Creative Commons licence, unless indicated otherwise in a credit line to the material. If material is not included in the article's Creative Commons licence and your intended use is not permitted by statutory regulation or exceeds the permitted use, you will need to obtain permission directly from the copyright holder. To view a copy of this licence, visit <http://creativecommons.org/licenses/by/4.0/>.

References

- Morgan RPC (2005) *Soil Erosion and Conservation* (3rd edition), Blackwell Publishing, USA
- Lim RP, Lee SW (1992) Hill development. Proceedings of the seminar; 1991Dec 1, Kuala Lumpur, Malaysian Nature Society, pp. 33–39
- Wajesundara NC, Abeysingha NS, Dissanayake DMSLB (2018) GIS-based soil loss estimation using RUSLE model: a case of Kirindi Oya river basin, Sri Lanka. *Model Earth Syst Environ* 4(1):251–262. <https://doi.org/10.1007/s40808-018-0419-z>
- Udayakumar EPN, Shrestha RP, Samarakoon L, Schimidt-Vogt D (2010) People's perception and socioeconomic determinants of soil erosion: a case study of Samanalawewa watershed, Sri Lanka. *Int J Sediment Res* 25(4):323–339. [https://doi.org/10.1016/S1001-6279\(11\)60001-2](https://doi.org/10.1016/S1001-6279(11)60001-2)
- Wischmeier WH, Smith DD (1978) Predicting rainfall erosion losses: a guide to conservation planning. Agriculture Handbook no 537. US Department of Agriculture, Science and Education Administration, Washington, DC, USA, p 163
- Remortel Van R, Hamilton M, Hickey R (2001) Estimating the LS factor for RUSLE through iterative slope length processing of digital elevation data. *Cartography* 30(1):27–35. <https://doi.org/10.1080/00690805.2001.9714133>
- Ganasri B, Ramesh H (2016) Assessment of soil erosion by RUSLE model using remote sensing and GIS-A case study of Nethravathi Basin. *Geosci Front* 7:953–961. <https://doi.org/10.1016/j.gsf.2015.10.007>
- Shinde V, Tiwari KN, Singh M (2010) Prioritization of micro watersheds on the basis of soil erosion hazard using remote sensing and geographic information system. *Int J Water Resour Environ Eng* 2(3):130–136
- Rozos D, Skilodimou HD, Loupasakis C, Bathrellos GD (2013) Application of the revised universal soil loss equation model on landslide prevention. An example is from N. Euboea (Evia) Island, Greece. *Environ Earth Sci* 70:3255–3266. <https://doi.org/10.1007/s12665-013-2390-3>
- Nakil M, Khire M (2016) Effect of slope steepness parameter computations on soil loss estimation: a review of methods using GIS. *Geocarto Int* 31(10):1078–1093. <https://doi.org/10.1080/10106049.2015.1120349>
- Zhao G, Kondolf GM, Mu X, Han M, He Z, Rubin Z, Wang F, Gao P, Sun W (2017) Sediment yield reduction associated with land-use changes and check dams in a catchment of the Loess Plateau, China. *CATENA* 148:126–137. <https://doi.org/10.1016/j.catena.2016.05.010>
- Wagari M, Taimur H (2021) RUSLE model-based annual soil loss quantification for soil erosion protection: a case of Fincha Catchment, Ethiopia. *Air Soil Water Res* 14:1–12. <https://doi.org/10.1177/11786221211046234>
- Thapa P (2020) Spatial estimation of soil erosion using RUSLE modeling: a case study of Dolakha district, Nepal. *Environ Syst Res* 9(15):1–10. <https://doi.org/10.1186/s40068-020-00177-2>
- Panditharathne DID, Abeysingha NS, Nirmanee KGS, Mallawantantri A (2019) Application of revised Universal Soil loss equation (rusle) model to assess soil erosion in Kalu Ganga River Basin in Sri Lanka. *Appl Environ Soil Sci*. <https://doi.org/10.1155/2019/4037379>
- Senanayake S, Pradhan B, Huete A, Brenan J (2020) Assessing soil Erosion hazards using land-use change and landslide frequency ratio Method: a case study of Sabaragamuwa Province, Sri Lanka. *Remote Sens* 12:1483. <https://doi.org/10.3390/rs12091483>
- Anees MT, Abdullah K, Nawawi MNM, Norulaini NAN, Syakir MI, Omar AKM (2018) Soil erosion analysis by RUSLE and sediment yield models using remote sensing and GIS in Kelantan state, Peninsular Malaysia. *Soil Res* 56:356–372. <https://doi.org/10.1071/SR17193>
- Azaiez N, Baazaoui N, Bhel IF, Hammami BS (2021) Contribution of the adjusted empirical analysis of the RSULE and FAO models in the estimation of soil losses in the watershed of Wadi El Hayat (Saudi Arabia). *Arab J Geosci* 14:2185. <https://doi.org/10.1007/s12517-021-08561-7>
- Kouli M, Soupios P, Valliantos F (2009) Soil erosion prediction using the revised Universal Soil loss equation in a GIS framework, Chania, Northwestern Crete, Greece. *Environ Geol* 57:483–497. <https://doi.org/10.1007/s00254-008-1318-9>
- Thomas J, Joseph S, Thrivikramji KP (2018) Assessment of soil erosion in a tropical mountain river basin of the southern

- Western Ghats, India, using RUSLE and GIS. *Geosci Front* 9:893–906. <https://doi.org/10.1016/j.gsf.2017.05.011>
20. Prasannakumar V, Shiny R, Geetha N, Vijith H (2011) Spatial prediction of soil erosion risk by remote sensing, GIS and RUSLE approach: a case study of Siruvani river watershed in Attapady valley, Kerala, India. *Environ Earth Sci* 64:965–972. <https://doi.org/10.1007/s12665-011-0913-3>
 21. Biswas SS, Pani P (2015) Estimation of soil erosion using RUSLE and GIS techniques: a case study of Baraka River Basin, Jharkhand, India. *Model Earth Syst Environ* 1(42):1–13. <https://doi.org/10.1007/s40808-015-0040-3>
 22. Mahala A (2019) Soil erosion estimation using RUSLE and GIS techniques—a study of a plateau fringe region of the tropical environment. *Arab J Geosci* 11(335):1–18. <https://doi.org/10.1007/s12517-018-3703-3>
 23. Jaiswal MK, Thakuria G, Borah AC, Saikia R (2014) Evaluation of parametric impact on soil loss of Panchnoi river basin, North-east India, using revised universal soil loss equation (rusle). *The Clarion* 3(1):51–60
 24. Dabral PP, Baithuri N, Pandey A (2007) Soil erosion assessment in a Hilly Catchment of North Eastern India using USLE, GIS, and remote sensing. *Water Resour Manage* 22:173–1798. <https://doi.org/10.1007/s11269-008-9253-9>
 25. Renard KG, Foster GR, Weesies GA, McCool DK, Yoder DC (1997) Predicting soil erosion by water: a guide to Conservation Planning with the revised Universal Soil loss equation (RUSLE). *Agriculture Handbook*, vol 703. US Department of Agriculture, Washington, DC, pp 1–251
 26. Bakis R, Bayajit Y, Ahmady DM, Cabuk SN (2021) Analysis and comparison of spatial rainfall distribution applying different interpolation methods in the porsuk river basin, Turkey. *Eskisehir Tech Univ J Sci Technol B-Theoretical Sci* 9(1):1–14. <https://doi.org/10.20290/estubtdb.726491>
 27. Ram B, Dhyani BL, Kumar N (2004) Assessment of erodibility status and refined Iso-Erodent Map of India. *Indian J soil Conserv* 32:171–177
 28. Stone RP, Hilborn D (2000) Universal Soil Loss Equation-Factsheet. <http://www.omafra.gov.on.ca/english/engineer/facts/00-001.htm>
 29. Moore ID, Burch GJ (1986) Physical basis of the length slope factor in the Universal Soil loss equation. *Soil Sci Soc Am* 50(5):1294–1298. <https://doi.org/10.2136/sssaj1986.036159950050000500>
 30. Weier J, Herring D (2000) Measuring vegetation (NDVI & EVI). NASA Earth Observatory, Washington DC
 31. Van der Knijff JM, Jones RJA, Montanarella L (2000) Soil Erosion Risk Assessment in Europe. EUR 19044 EN. Office for Official Publications of the European Communities, Luxembourg, p 34
 32. Zhou P, Luukkanen O, Tokola T, Nieminen J (2008) Effect of vegetation cover on soil erosion in a mountainous watershed. *CATENA* 75(3):319–325. <https://doi.org/10.1016/j.catena.2008.07.010>
 33. Pradhan B (2013) A comparative study on the predictive ability of the decision tree, support vector machine, and neuro-fuzzy models in landslide susceptibility mapping using GIS. *Comput Geosci* 51:350–365. <https://doi.org/10.1016/j.cageo.2012.08.023>
 34. Temesgen B, Mohammed MU, Korme T (2001) Natural hazard assessment using GIS and remote sensing methods, with particular reference to the landslides in the Wondogenet Area. *Ethiopia Phys Chem Earth Part C: Solar Terrestrial Planetary Sci* 26:665–675. [https://doi.org/10.1016/S1464-1917\(01\)00065-4](https://doi.org/10.1016/S1464-1917(01)00065-4)
 35. Uddin K, Matin MA, Maharjan SJS (2018) Assessment of land cover change and its impact on changes in soil erosion risk in Nepal. *Sustainability* 10(12):4715. <https://doi.org/10.3390/su10124715>
 36. Adornado HA, Yoshida M, Apolinar HA (2009) Erosion Vulnerability Assessment in REINA, Quezon Province, Philippines with Raster-based tool built within GIS environment. *Agric Inform Res* 18(1):24–31. <https://doi.org/10.3173/air.18.24>
 37. Prasannakumar V, Vijith H, Abinod NG (2012) Estimation of soil erosion risk within a small mountainous sub-watershed in Kerala, India, using revised Universal Soil loss equation (RUSLE) and geo-information technology. *Geosci Front* 3(2):209–215. <https://doi.org/10.1016/j.gsf.2011.11.003>
 38. Khosrokhani M, Pradhan B, Geomatics (2014) Natural Hazards and Risk, 5:3,252–270. Doi: <https://doi.org/10.1080/19475705.2013.794164>.
 39. George JK, Kumar S, Hole RM (2021) Geospatial modeling of soil erosion and risk assessment in indian Himalaya region-A study of Uttarakhand state. *Environ Adv* 4:100039. <https://doi.org/10.1016/j.envadv.2021.100039>
 40. FAO (2015) Global soil status, processes, and Trends. Status of the World's Soil Resources (SWSR)-Main report of the Food and Agriculture Organization. The Food and Agriculture Organization, Rome
 41. Tamene L, Le QB (2015) Estimating soil erosion in sub-saharan Africa based on landscape similarity mapping and using the revised universal soil loss equation (RUSLE). *Nutr Cycling Agroecosyst*. <https://doi.org/10.1007/s10705-10015-19674-10709>
 42. Imamoglu A, Dengiz O (2016) Determination of soil erosion risk using the RUSLE model and soil organic carbon loss in the Alaca catchment (Central Black Sea region, Turkey). *Rend Fis Acc Lincei*. <https://doi.org/10.1007/s12210-016-0556-0>
 43. Tang Q, Xu Y, Bennett SJ, Li Y (2015) Assessment of soil erosion using RUSLE and GIS: a case study of the Yangou watershed in the Loess Plateau, China. *Environ Earth Sci* 73:1715–1724. <https://doi.org/10.1007/s132665-014-3523-z>
 44. Yusof NF, Lihan T, Idris WMR, Rahman ZA, Mustapha MA, Yusof MAW (2019) Prediction of soil erosion in Pansoon Sub-basin, Malaysia using RUSLE integrated in geographical information system. *Sains Malays* 48(11):2565–2574. <https://doi.org/10.17576/jsm-2019-4811-26>

Publisher's Note Springer Nature remains neutral with regard to jurisdictional claims in published maps and institutional affiliations.